

⁶⁸Ga-Pentixafor PET/CT for Detection of Chemokine Receptor CXCR4 Expression in Myeloproliferative Neoplasms

Sabrina Kraus¹, Alexander Dierks^{2,3}, Leo Rasche¹, Olivia Kertels⁴, Malte Kircher^{2,3}, Andreas Schirbel², Josip Zovko¹, Torsten Steinbrunn¹, Raoul Tibes^{1,5}, Hans-Jürgen Wester⁶, Andreas K. Buck², Hermann Einsele¹, K. Martin Kortüm¹, Andreas Rosenwald⁷, and Constantin Lapa^{2,3}

¹Department of Internal Medicine II, University Hospital of Würzburg, Würzburg, Germany; ²Department of Nuclear Medicine, University Hospital of Würzburg, Würzburg, Germany; ³Nuclear Medicine, Medical Faculty, University of Augsburg, Augsburg, Germany; ⁴Department of Diagnostic Radiology, University Hospital of Würzburg, Würzburg, Germany; ⁵Division of Hematology and Medical Oncology, New York University School of Medicine, New York, New York; ⁶Pharmaceutical Radiochemistry, Technical University of Munich, Munich, Germany; and ⁷Institute of Pathology, University of Würzburg, Würzburg, Germany

C-X-C motif chemokine receptor 4 (CXCR4) is an attractive target for cancer diagnosis and treatment, as it is overexpressed in many solid and hematologic malignancies. This study investigated the feasibility of CXCR4-directed imaging with PET/CT using ⁶⁸Ga-pentixafor to visualize and quantify disease involvement in myeloproliferative neoplasms (MPNs). **Methods:** Twelve patients with MPNs (4 with primary myelofibrosis, 6 with essential thrombocythemia, and 2 with polycythemia vera) and 5 controls underwent ⁶⁸Ga-pentixafor PET/CT. Imaging findings were compared with immunohistochemical stainings, laboratory data, and splenic volume. **Results:** ⁶⁸Ga-pentixafor PET/CT was visually positive in 12 of 12 patients, and CXCR4 target specificity could be confirmed by immunohistochemical staining. A significantly higher tracer uptake could be detected in the bone marrow of MPN patients (SUV_{mean}, 6.45 ± 2.34 vs. 4.44 ± 1.24). Dynamic changes in CXCR4 expression determined by ⁶⁸Ga-pentixafor PET/CT corresponded with treatment response. **Conclusion:** ⁶⁸Ga-pentixafor PET/CT represents a novel diagnostic tool to noninvasively detect and quantify the extent of disease involvement in MPNs.

Key Words: myeloproliferative neoplasms; CXCR4; molecular imaging; PET; theranostics

J Nucl Med 2022; 63:96–99
DOI: 10.2967/jnumed.121.262206

Myeloproliferative neoplasms (MPNs) are a heterogeneous group of rare, potentially life-threatening hematopoietic stem cell disorders characterized by aberrant proliferation of one or more myeloid lineages (1). Because of similarities in pathogenesis and symptoms, diagnosis is often challenging. However, no imaging technique is presently established for the assessment of bone marrow (BM) involvement in MPNs

C-X-C motif chemokine receptor 4 (CXCR4) is a widely studied transmembrane chemokine receptor involved in tumor growth, metastasis, and hematopoietic stem cell or progenitor homing and retention in hematopoietic sites (2). In addition, previous studies

have shown CXCR4 overexpression in more than 30 different tumor entities (3–5), including multiple myeloma (6), diffuse large B-cell lymphoma (7), and small cell lung cancer (8). Recently, the radiolabeled CXCR4-targeted ligand ⁶⁸Ga-pentixafor has been developed for PET imaging and has been shown to noninvasively visualize CXCR4 expression in multiple hematologic malignancies as well as inflammatory disease conditions in vivo (3,5,7,9,10). However, there is limited knowledge regarding imaging features of MPNs.

The aim of this proof-of-principle study was to assess the feasibility of noninvasive CXCR4-directed imaging with PET/CT in patients with MPNs.

MATERIALS AND METHODS

Subjects and Study Design

Between April 2015 and May 2017, 12 patients (6 men and 6 women; age range, 37–73 y; mean age, 58.2 ± 9.1 y) with MPNs underwent molecular imaging with ⁶⁸Ga-pentixafor PET/CT. All patients had a clinically, molecularly, or histologically confirmed myeloproliferative disorder (primary myelofibrosis, *n* = 4; polycythemia vera, *n* = 2; essential thrombocythemia, *n* = 6). Detailed characteristics of the patient cohort are shown in Table 1. Five nononcologic patients (3 men and 2 women; mean age, 59 ± 8 y) were included as a control group (detailed in the supplemental methods; supplemental materials are available at <http://jnm.snmjournals.org>).

PET/CT Imaging

⁶⁸Ga-pentixafor was prepared as previously described (11) (detailed in the supplemental methods). After injection of ⁶⁸Ga-pentixafor (median, 130 MBq; range, 74–190 MBq), all PET/CT scans were performed on a dedicated PET/CT scanner (Biograph mCT 64; Siemens Medical Solutions) using standard acquisition and reconstruction protocols (detailed in the supplemental methods).

Image Analysis

PET/CT scans were visually assessed by 2 board-certified nuclear medicine physicians. First, a visual inspection of scans for elevated intramedullary tracer uptake (higher than mediastinal blood pool) was performed. For semiquantitative analysis, SUV_{mean} was determined as follows: in an initial step, transaxial slices in the middle of the L2–L4 vertebral bodies were selected. Next, tracer uptake in each vertebral body was determined by placing a region of interest of 10-mm diameter in the center of each vertebra. The individual overall SUV_{mean} (L2–L4) was calculated as the mean of the respective SUV_{mean} of

Received Feb. 27, 2021; revision accepted Apr. 1, 2021.
For correspondence or reprints, contact: Constantin Lapa (constantin.lapa@uk-augsburg.de).
*Contributed equally to this work.
Published online May 28, 2021.
COPYRIGHT © 2022 by the Society of Nuclear Medicine and Molecular Imaging.

TABLE 1
Patient Characteristics

Patient no.	Sex	Age (y)	Diagnosis	Disease stage	Mutation	Splenomegaly and splenic volume	Treatment	Follow-up PET/CT	CSCR4 IHC staining
1	M	73	PV	Initial diagnosis	JAK2 V617F	Yes (532 cm ³)	Ruxolitinib	Yes	Yes
2	F	66	ET	Initial diagnosis	JAK2 V617F	No (226 cm ³)	None	No	Yes
3	M	37	ET	Initial diagnosis	CALR	Yes (260 cm ³)	None	No	Yes
4	F	51	ET	Stable disease	JAK2 V617F	No (228 cm ³)	Anagrelide	No	Yes
5	M	60	ET	Initial diagnosis	CALR	Yes (450 cm ³)	Hydroxyurea	Yes	Yes
6	M	64	PMF	Initial diagnosis	JAK2 V617F	Yes (689 cm ³)	Ruxolitinib	Yes	Yes
7	M	58	PV	Stable disease	JAK2 V617F	No (280 cm ³)	Hydroxyurea	No	Yes
8	F	62	PMF	Progressive disease	JAK2 V617F	Yes (508 cm ³)	Ruxolitinib	No	Yes
9	F	42	PMF	Initial diagnosis	None detected	No (250 cm ³)	None	No	No
10	F	63	ET	Stable disease	JAK2 V617F	Yes (625 cm ³)	Hydroxyurea	No	No
11	M	58	PMF	Initial diagnosis	JAK2 V617F	No (214 cm ³)	None	No	Yes
12	F	52	ET	Stable disease	None detected	No (180 cm ³)	Anagrelide	No	No

IHC = immunohistochemistry; PV = polycythemia vera; ET = essential thrombocythemia; PMF = primary myelofibrosis; CALR = calreticulin.

these 3 regions of interest. For assessment of the spleen, a region of interest with a diameter of 4 cm was used. Background activity was measured by placing a 15-mm region of interest in the center of the right atrium (blood pool SUV). Mean tumor-to-blood ratios were calculated by dividing the L2–L4 SUV_{mean} by the blood pool SUV. Splenic volumes were assessed by means of CT.

Immunohistochemistry Stainings of Patient Biopsy Material

Immunohistochemistry stainings were performed on 10% formalin-fixed, paraffin-embedded BM biopsy samples from 9 of 12 MPN patients (detailed in the supplemental methods).

Statistical Analysis

Statistical analyses were performed using Prism software (version 6.0; GraphPad Software, Inc.). Results are shown as mean ± SD or median and range as indicated. All statistical tests were performed 2-sided, and a *P* value of less than 0.05 was considered to indicate statistical significance.

RESULTS

CXCR4-directed PET imaging with ⁶⁸Ga-pentixafor was visually positive in all patients. ⁶⁸Ga-pentixafor PET/CT depicted significantly increased tracer uptake both in the BM and in extramedullary hematopoietic sites as compared with

controls, with an SUV_{mean} of 4.44 ± 1.3 in the BM (controls, 2.67 ± 0.41; *P* = 0.01) and an SUV_{mean} of 6.45 ± 2.34 in the spleen (controls, 4.44 ± 1.24; *P* = 0.09) (example given in Fig. 1). Individual imaging results can be found in Supplemental Tables 1 and 2, respectively.

No significant differences were observed between the SUV_{mean} of the different subtypes of MPN (Table 2). Patients with JAK2V617F-positive or CALR-positive mutations did not show higher BM uptake than JAK2V617F-negative patients (*r* = 0.19, *P* = not statistically significant). Additional BM biopsies were available in 9 of 12 patients and confirmed moderate to strong CXCR4 expression in dysplastic cells of the megakaryocytic lineage in all samples (Supplemental Fig. 1).

Three patients additionally underwent follow-up CXCR4-directed PET/CT after a median of 6 mo (range, 4–7 mo) after treatment initiation with ruxolitinib (patients 1 and 6) and hydroxyurea (patient 5). In these patients, initially high tracer accumulation in the spleen and BM (with an SUV_{mean} of 6.12 ± 2.15, 3.60 ± 1.14, and 4.10 ± 0.32, respectively) declined (SUV_{mean}: BM, 3.97 vs. 2.86; spleen, 7.72 vs. 4.89) in response to treatment (Fig. 2). Furthermore, the decrease in SUV_{mean} after treatment corresponded with a spleen volume reduction and normalization of hemoglobin, peripheral leukocyte count,

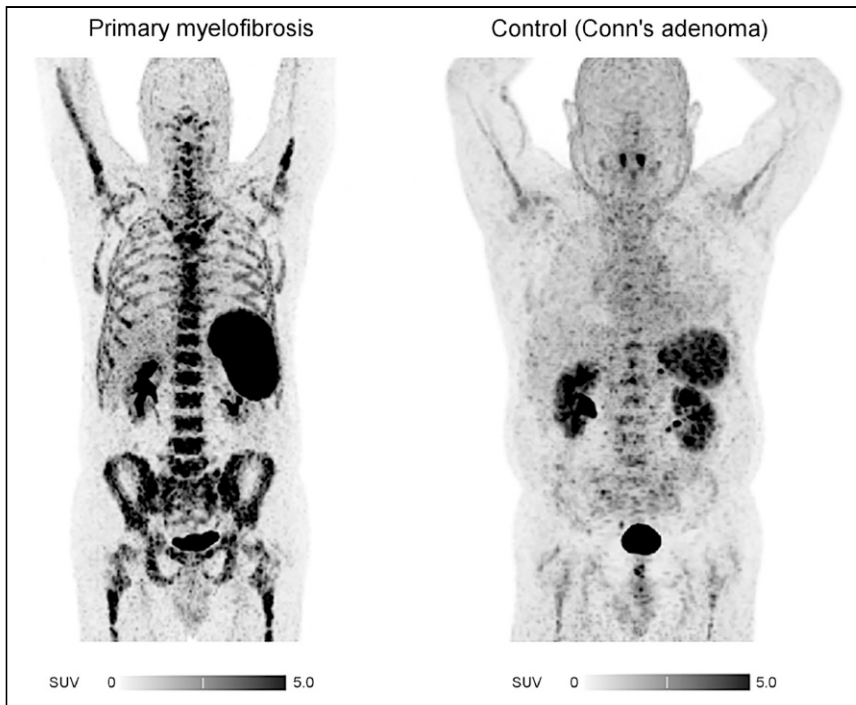


FIGURE 1. Display of patient (patient 6) with primary myelofibrosis. ^{68}Ga -pentixafor PET/CT (maximum-intensity projections) depicts significantly increased tracer uptake in BM as well as spleen compared with control group.

thrombocyte count, and lactate dehydrogenase level (Supplemental Table 2).

DISCUSSION

Although PET/CT imaging is widely used for the diagnosis, staging, and response assessment of various types of hematologic malignancies (12), it is not routinely used in patients with MPNs. Currently, with the diagnosis being based solely on the assessment of clinical, hematologic, histopathologic, and genetic parameters (1), no imaging technique is established for the assessment of BM involvement. Here, we present the first (to our knowledge) proof-of-principle study investigating the *in vivo* application of ^{68}Ga -pentixafor in patients with MPNs. We demonstrate the feasibility of ^{68}Ga -pentixafor PET/CT to noninvasively detect and quantify the extent of BM involvement, with MPN patients demonstrating significantly higher tracer uptake in the BM and extramedullary hematopoietic sites than was seen in nonmalignant controls. With SUV_{mean} ranging between 2.9 and 7.4, the intensity of ^{68}Ga -

pentixafor uptake in the BM of MPN patients was similar to that previously reported for BM involvement in patients with chronic lymphatic leukemia (13) and acute myeloid leukemia (14).

Interestingly, in our small cohort, the highest tracer accumulation was detected in the BM of a patient with essential thrombocythemia at the time of initial diagnosis. However, further research to establish and validate cutoffs for both detection of BM involvement and differentiation between various disease types is still needed.

Our findings are consistent with the concept of MPNs as chronic inflammatory diseases (15) in conjunction with an impaired microenvironment that favors malignant over normal hematopoiesis through profound changes in the BM stromal compartment and increased cytokine levels. Interestingly, megakaryocytes have been shown to contribute to MPN pathology and to be a major driver of BM fibrosis (16). In line with that observation, our immunohistochemistry data show CXCR4 expression predominantly on the surface of dysplastic cells of the megakaryocytic lineage. In this

context, the extent of CXCR4 uptake may, therefore, also serve as a prognostic factor to further stratify MPN patients.

We monitored 3 newly diagnosed MPN patients (3 of our total of 12 patients) over a median of 6 mo after treatment initiation, showing that CXCR4 uptake determined by ^{68}Ga -pentixafor PET/CT might correlate with treatment response. The extent of both BM and splenic uptake (SUV_{mean} : BM, 3.97 vs. 2.86; spleen, 7.72 vs. 4.89) decreased with treatment initiation. Interestingly, tracer uptake in BM and spleen corresponded with hematologic parameters and splenic volume. The reduction in SUV_{mean} after treatment correlated with normalization of hemoglobin, peripheral leukocyte count, thrombocyte count, and lactate dehydrogenase. Whereas recent data suggest additional utility for CXCR4-directed PET/CT imaging for response assessment in hematologic malignancies such as extranodal marginal zone lymphoma (17) or central nervous system B-cell lymphoma (18), the extent to which ^{68}Ga -pentixafor PET/CT can be used for response assessment in MPNs needs to be investigated in future prospective studies.

TABLE 2
BM CXCR4 and Splenic Uptake in MPNs

Parameter	All patients (n = 12)	Primary myelofibrosis (n = 4)	Essential thrombocythemia (n = 6)	Polycythemia vera (n = 2)	Controls (n = 5)
BM SUV_{mean}	4.44 ± 1.3 (2.9–7.4)	5.48 ± 0.80 (4.2–6.1)	4.01 ± 1.40 (2.9–7.4)	3.92 ± 0.22 (3.7–4.1)	2.67 ± 0.41 (2.3–3.3)
Spleen SUV_{mean}	6.45 ± 2.34 (3.5–12.5)	6.12 ± 0.76 (4.6–6.4)	7.37 ± 2.53 (4.1–12.5)	4.72 ± 1.25 (3.5–6.0)	4.44 ± 1.24 (2.9–5.4)

Data are SUV_{mean} . Values are provided as mean ± SD (range).

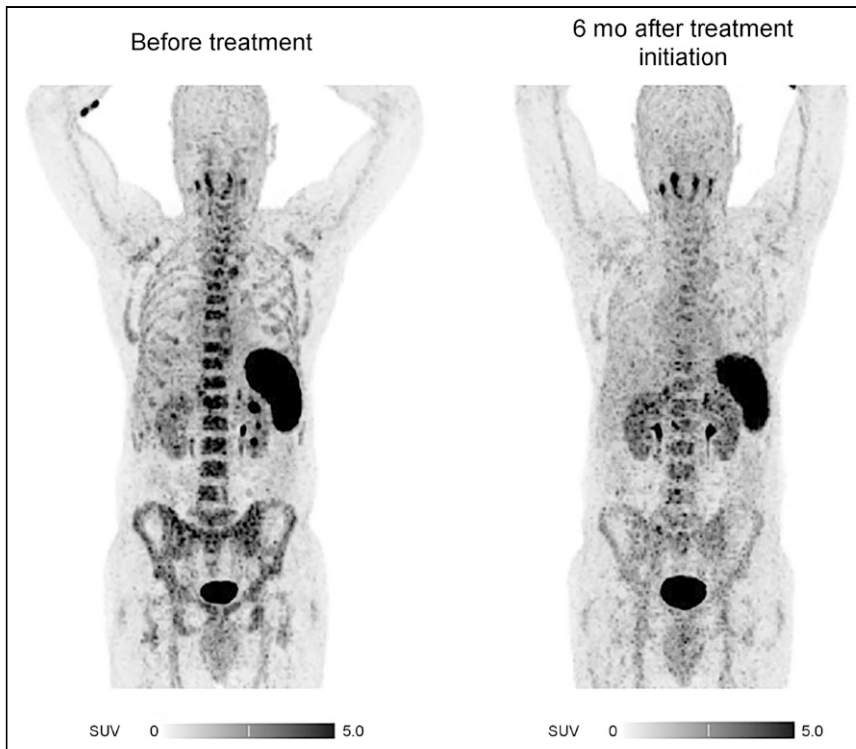


FIGURE 2. Response assessment with CXCR4-directed PET/CT imaging (maximum-intensity projections). Shown is example of therapy-induced CXCR4 downregulation in patient with essential thrombocythemia (patient 5).

Our pilot observation suffers from several limitations. The radiation exposure associated with PET/CT prevented the use of a control group of healthy individuals. Instead, we included Conn adenoma patients as a control group who received CXCR4 PET/CT imaging as part of their endocrinologic investigation (19), and ^{68}Ga -pentixafor uptake in other controls might be even lower than in our endocrinologic control group. However, when compared with previously reported upper limits of physiologic BM uptake measurements in cancer patients without BM involvement, values agree broadly with our study (SUV_{mean} : BM for pancreatic adenocarcinoma, 1.7; BM for mucosa-associated lymphoid tissue lymphoma, 2.3) (13). Furthermore, although immunohistochemical analysis could demonstrate CXCR4 expression in all BM biopsies, CXCR4 expression was relatively low and did not clearly correspond with the intensity of the PET signal. However, surface expression of CXCR4 is a dynamic process and can be influenced by therapeutic interventions (20).

CONCLUSION

To our knowledge, our data are the first to demonstrate that CXCR4-directed imaging with ^{68}Ga -pentixafor PET/CT is feasible to visualize and quantify disease involvement in MPN patients. Further evaluation in larger, prospective studies is warranted to determine the clinical impact in primary staging and response assessment and to evaluate the potential for a theranostic approach.

DISCLOSURE

Hans-Jürgen Wester is the founder and shareholder of Scintomics. No other potential conflict of interest relevant to this article was reported.

KEY POINTS

QUESTION: Is CXCR4-directed PET imaging with ^{68}Ga -pentixafor feasible to visualize and quantify disease involvement in MPNs?

PERTINENT FINDINGS: This retrospective analysis revealed that CXCR4-directed imaging is positive in all investigated patients and showed a significantly higher tracer uptake in the BM of patients with MPNs.

IMPLICATIONS FOR PATIENT CARE: CXCR4-directed PET imaging with ^{68}Ga -pentixafor is feasible to noninvasively detect and quantify the extent of BM involvement in patients with MPNs.

REFERENCES

- Spivak JL. Myeloproliferative neoplasms. *N Engl J Med*. 2017;377:895–896.
- Jacobson O, Weiss ID. CXCR4 chemokine receptor overview: biology, pathology and applications in imaging and therapy. *Theranostics*. 2013;3:1–2.
- Zhao H, Guo L, Zhao H, Zhao J, Weng H, Zhao B. CXCR4 over-expression and survival in cancer: a system review and meta-analysis. *Oncotarget*. 2015; 6:5022–5040.
- Domanska UM, Kruizinga RC, Nagengast WB, et al. A review on CXCR4/CXCL12 axis in oncology: no place to hide. *Eur J Cancer*. 2013;49:219–230.
- Kircher M, Herhaus P, Schottelius M, et al. CXCR4-directed theranostics in oncology and inflammation. *Ann Nucl Med*. 2018;32:503–511.
- Lapa C, Schreder M, Schirbel A, et al. [^{68}Ga]pentixafor-PET/CT for imaging of chemokine receptor CXCR4 expression in multiple myeloma: comparison to [^{18}F]FDG and laboratory values. *Theranostics*. 2017;7:205–212.
- Lapa C, Hanscheid H, Kircher M, et al. Feasibility of CXCR4-directed radioligand therapy in advanced diffuse large B-cell lymphoma. *J Nucl Med*. 2019;60:60–64.
- Lapa C, Luckerath K, Rudelius M, et al. [^{68}Ga]pentixafor-PET/CT for imaging of chemokine receptor 4 expression in small cell lung cancer: initial experience. *Oncotarget*. 2016;7:9288–9295.
- Derlin T, Hueper K. CXCR4-targeted therapy in breast cancer. *Lancet Oncol*. 2018;19:e370.
- Reiter T, Kircher M, Schirbel A, et al. Imaging of C-X-C motif chemokine receptor CXCR4 expression after myocardial infarction with [^{68}Ga]pentixafor-PET/CT in correlation with cardiac MRI. *JACC Cardiovasc Imaging*. 2018;11:1541–1543.
- Martin R, Juttler S, Muller M, Wester HJ. Cationic eluate pretreatment for automated synthesis of [^{68}Ga]CPC4.2. *Nucl Med Biol*. 2014;41:84–89.
- Valls L, Badve C, Avril S, et al. FDG-PET imaging in hematological malignancies. *Blood Rev*. 2016;30:317–331.
- Mayerhoefer ME, Jaeger U, Staber P, et al. [^{68}Ga]Ga-pentixafor PET/MRI for CXCR4 imaging of chronic lymphocytic leukemia: preliminary results. *Invest Radiol*. 2018;53:403–408.
- Herhaus P, Habringer S, Philipp-Abbrederis K, et al. Targeted positron emission tomography imaging of CXCR4 expression in patients with acute myeloid leukemia. *Haematologica*. 2016;101:932–940.
- Longhitano L, Li Volti G, Giallongo C, et al. The role of inflammation and inflammasome in myeloproliferative disease. *J Clin Med*. 2020;9:2334.
- Ciurea SO, Merchant D, Mahmud N, et al. Pivotal contributions of megakaryocytes to the biology of idiopathic myelofibrosis. *Blood*. 2007;110:986–993.
- Herhaus P, Habringer S, Vag T, et al. Response assessment with the CXCR4-directed positron emission tomography tracer [^{68}Ga]pentixafor in a patient with extranodal marginal zone lymphoma of the orbital cavities. *EJNMMI Res*. 2017;7:51.
- Herhaus P, Lipkova J, Lammer F, et al. CXCR4-targeted PET imaging of central nervous system B-cell lymphoma. *J Nucl Med*. 2020;61:1765–1771.
- Rieckmann M, Delgobo M, Gaal C, et al. Myocardial infarction triggers cardioprotective antigen-specific T helper cell responses. *J Clin Invest*. 2019;129:4922–4936.
- Lapa C, Luckerath K, Kircher S, et al. Potential influence of concomitant chemotherapy on CXCR4 expression in receptor directed endoradiotherapy. *Br J Haematol*. 2019;184:440–443.